Materials Science & Engineering A 729 (2018) 141–148

Contents lists available at ScienceDirect

Materials Science & Engineering A

journal homepage: www.elsevier.com/locate/msea

Microstructure and properties of bulk $Al_{0.5}CoCrFeNi$ high-entropy alloy by cold rolling and subsequent annealing

Tong Guo[a], Jinshan Li[a,*], Jun Wang[a,*], William Yi Wang[a], Yi Liu[b], Ximing Luo[b], Hongchao Kou[a], Eric Beaugnon[c,d]

[a] State Key Laboratory of Solidification Processing, Northwestern Polytechnical University, Xi'an, Shaanxi 710072, PR China
[b] State Key Laboratory of Advanced Technologies for Comprehensive Utilization of Platinum Metals, Kunming Institute of Precious Metals, Kunming 650106, PR China
[c] Univ. Grenoble Alps, LNCMI, F-38000 Grenoble, France
[d] CNRS, LNCMI, F-38000 Grenoble, France

ARTICLE INFO

Keywords:
High-entropy alloy
Cold-rolling
Recrystallization
Mechanical properties

ABSTRACT

Cold rolling combining subsequent annealing is implemented to tune the microstructure and mechanical properties of $Al_{0.5}CoCrFeNi$ high-entropy alloy. Results show that the microstructure of $Al_{0.5}CoCrFeNi$ HEA after 80% thickness reduction is severely deformed along the rolling direction. Prominent work hardening effect on $Al_{0.5}CoCrFeNi$ HEAs is evidenced by the remarkable enhancement of the hardness and strength at the sacrifice of ductility. After annealing, detailed description of microstructure evolution, texture analyses as well as tensile properties are given. Strongly temperature dependent recrystallized microstructure manifests the rather high recrystallization temperature (0.81 T_m) that can be attributed to original coarse as-cast grains, severe lattice distortion effect and sluggish diffusion effect. Progressively smaller intensity of deformed texture proves the function to eliminate texture effectively of recrystallization in spite of the detection of weak recrystallization texture. Tensile tests of annealed $Al_{0.5}CoCrFeNi$ HEAs show the strength decreases dramatically while ductility increases remarkably accompanying increased annealing temperature. To sum up, cold rolling combining subsequent annealing is a valid method to gain grain refined $Al_{0.5}CoCrFeNi$ HEAs with adjustable properties that are prospective for many kinds of application.

1. Introduction

High-entropy alloys (HEAs) are originally defined by Yeh [1] as containing five or more principal elements in equal or near equal atomic percent [2–4]. Despite having the presence of a large number of components, the HEAs generally show simple solid-solution structures rather than complicated intermetallic compounds [1], which are characterized in forms of FCC, BCC, FCC + BCC or HCP structure [4–7]. HEAs also possess attractive properties according recent extensive research such as great integrated tensile properties in a wide temperature range [8–15], high hardness [16], superior wear-resistance [17,18], good corrosion-resistance and thermal stability [19,20], making HEAs prospective for engineering application [20–22]. As a result, preparation of bulk HEAs and improving the mechanical properties have been the most interesting fields for many researchers.

Nevertheless, as-cast alloys are usually unsuitable for the study of mechanical properties on account of the existence of inevitable cast defects which would develop into cracks and result in the premature failure of the materials. In addition, coarse microstructure produced during casting is also disastrous for the mechanical properties. Researchers usually adopt cold rolling and/or heat treatment to eliminate cast defects as well as tune microstructure before conducting the research. P.P. Bhattacharjee et al. [23] reported that homogenized CoCrFeMnNi HEAs was cold-rolled to ~ 50% reduction in thickness and then annealed at 800 °C for 1 h so as to break down the cast structure. These fully annealed samples were used as their starting materials for subsequent experiment. Sun et al. [24] successfully obtained fully recrystallized CoCrFeMnNi HEAs with different grain sizes and studied the Hall-Petch relationship. Ma et al. [25] employed homogenized, cold-rolled and annealed $Al_{0.6}CoCrFeNi$ HEAs as the research object. Although cold rolling combining subsequent annealing plays an important role in the tuning of microstructure as well as enhancement of mechanical properties [26–30], comprehensive investigation about the effect of cold rolling combining subsequent annealing on HEAs is still insufficient. Hence, $Al_{0.5}CoCrFeNi$ high-entropy alloy is cold-rolled and annealed in this work to inspect the corresponding changes of

* Corresponding authors.
E-mail addresses: ljsh@nwpu.edu.cn (J. Li), nwpuwj@nwpu.edu.cn (J. Wang).

https://doi.org/10.1016/j.msea.2018.05.054
Received 23 January 2018; Received in revised form 15 May 2018; Accepted 16 May 2018
Available online 17 May 2018
0921-5093/

microstructure and mechanical properties.

2. Experimental procedures

A small $Al_{0.5}CoCrFeNi$ HEA ingots weighing about 30 g is prepared by arc-melting under argon atmosphere with high purity Al, Co, Cr, Fe and Ni (purities higher than 99.9 wt.%). The ingot is re-melted for four times to achieve homogenous elements distribution. Then a sample with a weight of 40 mg prepared for DSC analysis (Q1000 DSC) is cut from the small ingot. The DSC experiment temperature is raised to 1450 °C to detect the melting point under argon atmosphere at a rate of 10 °C/min. Then, Al, Co, Cr, Fe and Ni with purity higher than 99.9 wt. % are used to prepare the HEA with vacuum induction-melting furnace. The furnace is heated to 500 °C and held for 2 h to remove the water vapor. After the vacuum of induction-melting furnace reached 10 Pa, pure argon is backfilled to expel the rest of air until the vacuum goes back to atmospheric pressure. This process is repeated 3 times in order to gain oxygen-free environment as much as possible. Melting and casting is performed in a vacuum of 0.05 MPa by backfilling with high purity argon and the liquid metal is held at about 1550 °C for 15 min. Approximately 15.8 kg master alloy is casted into a steel crucible with a length of 180 mm, upper inner diameter of 140 mm and bottom inner diameter of 130 mm. The DSC curve shows the melting point of as-cast $Al_{0.5}CoCrFeNi$ HEA is 1358 °C so the induction heating process under 1550 °C is reasonable.

Two specimens with dimensions 70 mm (length) × 20 mm (width) × 8 mm (thickness) are obtained from the same position of as-cast ingot to reduce the cooling-rate effect. Further considering the small volume of these two specimens, the cooling-rate effect can be ignored. One specimen is used as the as cast condition and the other is cold rolled to a thickness reduction of 80%. The 80% CR specimen is annealed at 700 °C, 800 °C, 900 °C, 1000 °C, 1100 °C and 1200 °C for one hour. Microstructure of the cast, cold-rolled and annealed alloys is studied from the longitudinal plane (RD × ND plane) by A MIRA3 XMU scanning electron microscope (SEM) equipped with a Nordlys Max EBSD detector and the EBSD maps are analyzed by TSLOIM EBSD software. In the EBSD maps, black and white lines represent the HAGBs and LAGBs respectively. Standard bright-field images are obtained with a FEI Tecnai G2 F30 Transmission Electron Microscope (TEM). The crystalline structure is characterized by a DX-2700 X-ray diffraction instrument. The hardness values is measured with a Vickers hardness tester under a load of 1 kg and a holding time of 15 s. Dog bone-shaped tensile specimens are prepared along the RD direction for room temperature tensile test with a gauge length of 14 mm, a width of 2 mm and a thickness around 1.5 mm. Uniaxial tensile tests are carried out with a MTS SANS CMT5105 testing machine at room temperature with strain rate of 10^{-3} s^{-1}.

3. Results and discussion

3.1. DSC analysis

DSC experiment is carried out and the curve during heating is presented in Fig. 1. A remarkable endothermic peak represent the melting point is found at the temperature of 1358 °C. The melting point is used as the reference for preparation of bulk ingots and re-crystallization temperature that will be discussed later.

3.2. Microstructure after cold rolling processing

Fig. 2 shows the XRD patterns of the as-cast and the cold-rolled alloys. All alloys exhibit a mixture of FCC and BCC crystalline structures, while FCC is the dendritic phase and BCC is interdendritic phase. The lattice parameters of FCC are calculated to be 0.3606 nm and 0.3628 nm for the as-cast and 80% CR conditions respectively, indicating the severe lattice distortion under plastic deformation.

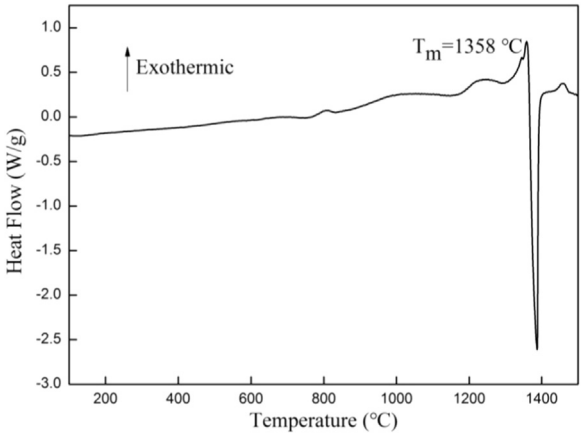

Fig. 1. DSC curve of as-cast $Al_{0.5}CoCrFeNi$ HEA.

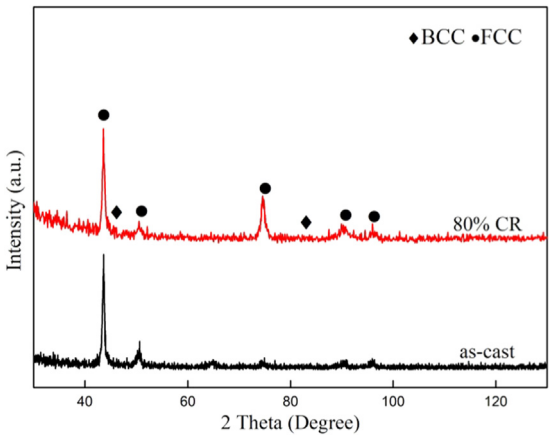

Fig. 2. The XRD patterns of the $Al_{0.5}CoCrFeNi$ high-entropy alloys at as-cast and 80% CR conditions.

Fig. 3 shows the SEM micrographs of $Al_{0.5}CoCrFeNi$ alloys in both as-cast and cold-rolled statuses. The as-cast microstructure is typical dendrite morphology with interdendritic BCC phase and matrix FCC phase [31,32]. The chemical composition (atomic percent) of $Al_{0.5}CoCrFeNi$ HEA in dendrite and interdendritic regions measured by EDS are listed in Table 1. It shows that the dendrite matrix FCC phase is enriched with Cr and Fe and depleted in Al and Ni, while opposite elemental distribution is presented in the interdendritic BCC phase, and Co is relatively homogeneous in both phases. The coarse grains are elongated and severely-deformed microstructure along the rolling direction can be observed (Fig. 3(b)). In order to facilitate observation of the microstructure, the rolling direction is pointed by red arrow in Fig. 3(b).

3.3. Mechanical properties after cold rolling processing

Fig. 4(a) shows the tensile engineering stress-strain curves of $Al_{0.5}CoCrFeNi$ HEAs at as-cast and 80% CR conditions. The ultimate tensile strength, yield strength and uniform elongation of as-cast alloy are 568 MPa, 402 MPa and 33.68%, respectively. The 80% CR condition demonstrates large yield strength of 1396 MPa but very limited uniform elongation of 5.37%. Both the yield strength and tensile strength increase dramatically accompanying with the rolling processing at the sacrifice of the ductility, and the yield strength is more than three times higher after 80% CR while plasticity is not completely lost. The microhardness of these two statuses is also presented in Table 2. Hardness achieved by 80% CR reduction in this work is 480 HV, 2.67 times higher than the as-cast condition (180 HV). The significant

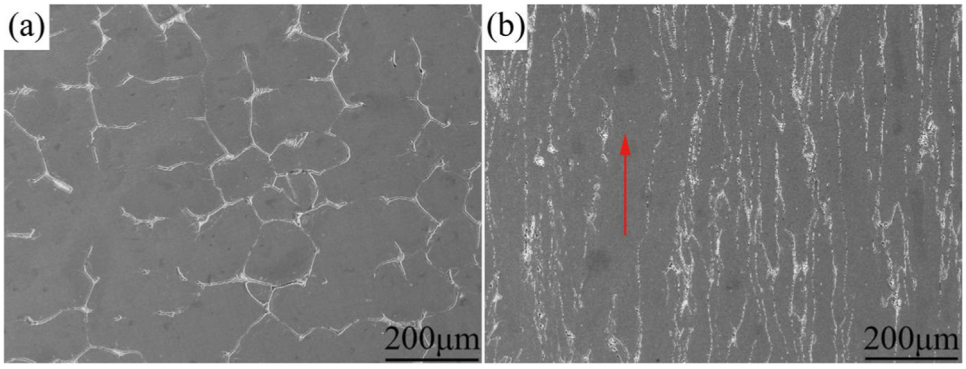

Fig. 3. Microstructures of the $Al_{0.5}CoCrFeNi$ high-entropy alloys at as-cast and 80% CR conditions. (Red arrow represents the rolling direction). (For interpretation of the references to color in this figure legend, the reader is referred to the web version of this article.).

Table 1
The chemical composition (atomic percent) of $Al_{0.5}CoCrFeNi$ HEA in dendrite and interdendritic regions.

Element	Al	Co	Cr	Fe	Ni
Nominal	11.11	22.22	22.22	22.22	22.22
Dendrite	9.36	21.80	23.50	23.86	21.48
Interdendritic	14.82	22.37	18.71	18.56	25.54

Table 2
Mechanical properties of as-cast and cold-rolled $Al_{0.5}CoCrFeNi$ HEAs.

Cold reduction	σ_y [MPa]	σ_u [MPa]	ε_u [%]	Hardness [HV]
0	402	568	33.68	180
80%	1396	1461	5.37	480

enhancement of strength and micro-hardness reveals arresting work hardening effect of cold-rolling on $Al_{0.5}CoCrFeNi$ HEAs.

3.4. Work hardening analysis

From Fig. 4(a) and Table 2, noteworthy enhancement of hardness, yield strength and tensile strength obtained by CR can be observed, which has also been reported in other HEAs [33,34]. Work hardening from dislocation-based activities such as accumulation of dislocation density and forming dislocation network during cold rolling process is the main factor for this phenomenon. Commonly, the dislocation density ρ can be up to 10^{12} dislocations per cm^2 for a plastically cold-rolled metal and the flow stress τ is approximately proportional to the square root of dislocation density [35–37]:

$$\tau = \tau_0 + \alpha G b \sqrt{\rho} \quad (1)$$

where τ_0 is the initial stress necessary to move a dislocation in the absence of other dislocations, α is a constant between 0.3 and 0.6, G is the shear modulus and b is the Burgers vector. As is known to all, increasing of thickness reduction leads to the dislocation multiplication and then interactions between dislocations ultimately enlarge the resistance of dislocation motion in the progress of deformation. In general, a higher dislocation density leads to a higher strength [29]. As illustrated by white arrows in Fig. 4(b), closely packed dense dislocation cells [38] caused by movement and interaction of dislocation are observed with TEM in the cold-rolled sample. Thus, $Al_{0.5}CoCrFeNi$ HEA appears extremely significant strengthening by cold-rolling. Meanwhile, F. Otto et al. [39] recently reported that the deformation twinning in CoCrFeMnNi high-entropy alloy introduces extra interfaces within the grains during deformation ("dynamic Hall-Petch") hence the work hardening rate and the ultimate tensile strength are increased. Gludovatz et al. [40] have substantiated that mechanical nano-twinning makes contribution to the mechanical properties improvement of CoCrFeMnNi HEA at cryogenic temperature. The twinning may also generate during the deformation process of $Al_{0.5}CoCrFeNi$ HEAs and plays a significant role in the increase of hardness and strength. In addition, as stated in the XRD analysis (see Fig. 2), micro-strain caused by cold deformation enhances the lattice distortion, which also contributes to the strengthening [36].

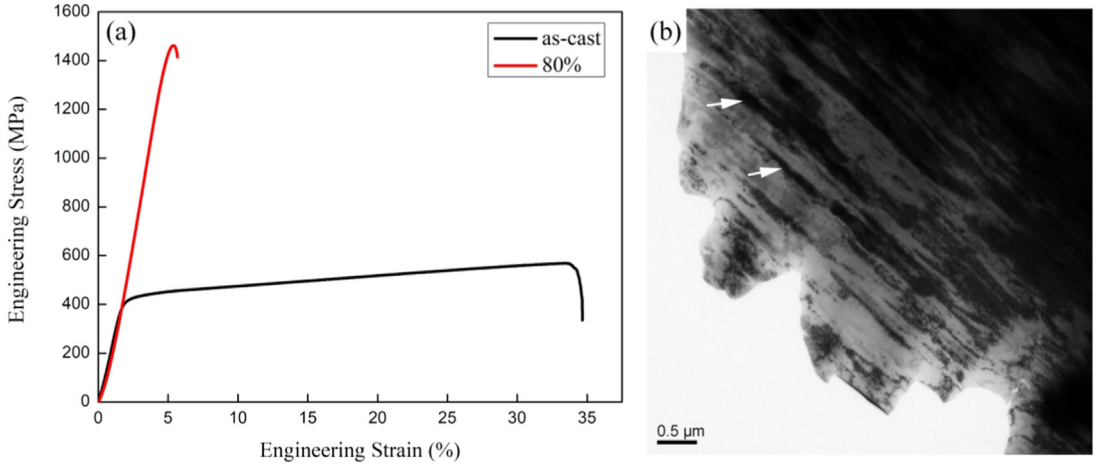

Fig. 4. (a) Engineering stress-strain curves of $Al_{0.5}CoCrFeNi$ HEAs at as-cast and 80% CR conditions; (b) bright-field image of $Al_{0.5}CoCrFeNi$ HEA at 80% CR condition.

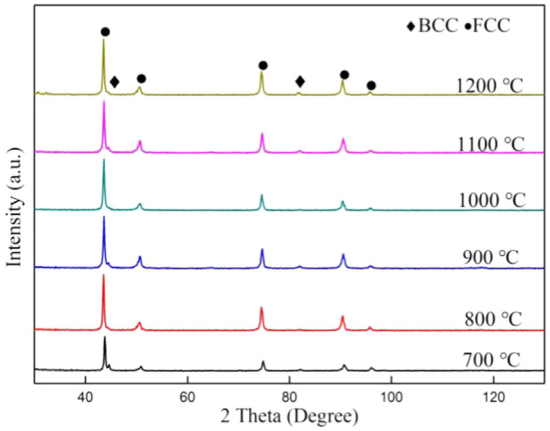

Fig. 5. The XRD patterns of $Al_{0.5}CoCrFeNi$ HEAs annealed at different temperature.

3.5. Microstructure after annealing treatment

Annealing is performed to cold rolled samples in order to tune the microstructure and mechanical properties through recrystallization that is feasible in other alloys [26–30]. Fig. 5 shows the XRD patterns for $Al_{0.5}CoCrFeNi$ HEAs with 80% rolling reduction during the isochronal annealing at different temperature. All alloys after annealing still consist of FCC and BCC phases, which is the same with as-cast and cold-rolled samples in Fig. 2.

Fig. 6 shows detailed microstructure evolution from partial recrystallization to fully recrystallization and it's clearly that the microstructure is strongly temperature dependent. The alloy heat-treated at 900 °C exhibits partially refined recrystallized microstructure during the grain boundaries as well as phase interface and areas in large portion maintain the deformed morphology covered with profuse LAGBs (Fig. 6(a)). The microstructure indicates that recrystallization nucleation is preferred in the grain boundaries and phase interface with high dislocation density induced by cold rolling. After annealing at 1000 °C, the IPF map in Fig. 6(b) shows enlarged recrystallized areas but still some original deformed microstructure. When the annealing temperature continues to rise, deformed microstructure is gradually replaced by refined equiaxed recrystallization grains and fully recrystallization microstructure is obtained after annealing at 1200 °C (Fig. 6(d)). The grain sizes for the alloy annealed at 1200 °C are mainly distributed around 0.75 μm ~ 4 μm according to statistics of grain sizes distribution in Fig. 7. Comparing with the as-cast condition, remarkable grains refinement is achieved through annealing treatment. Such a

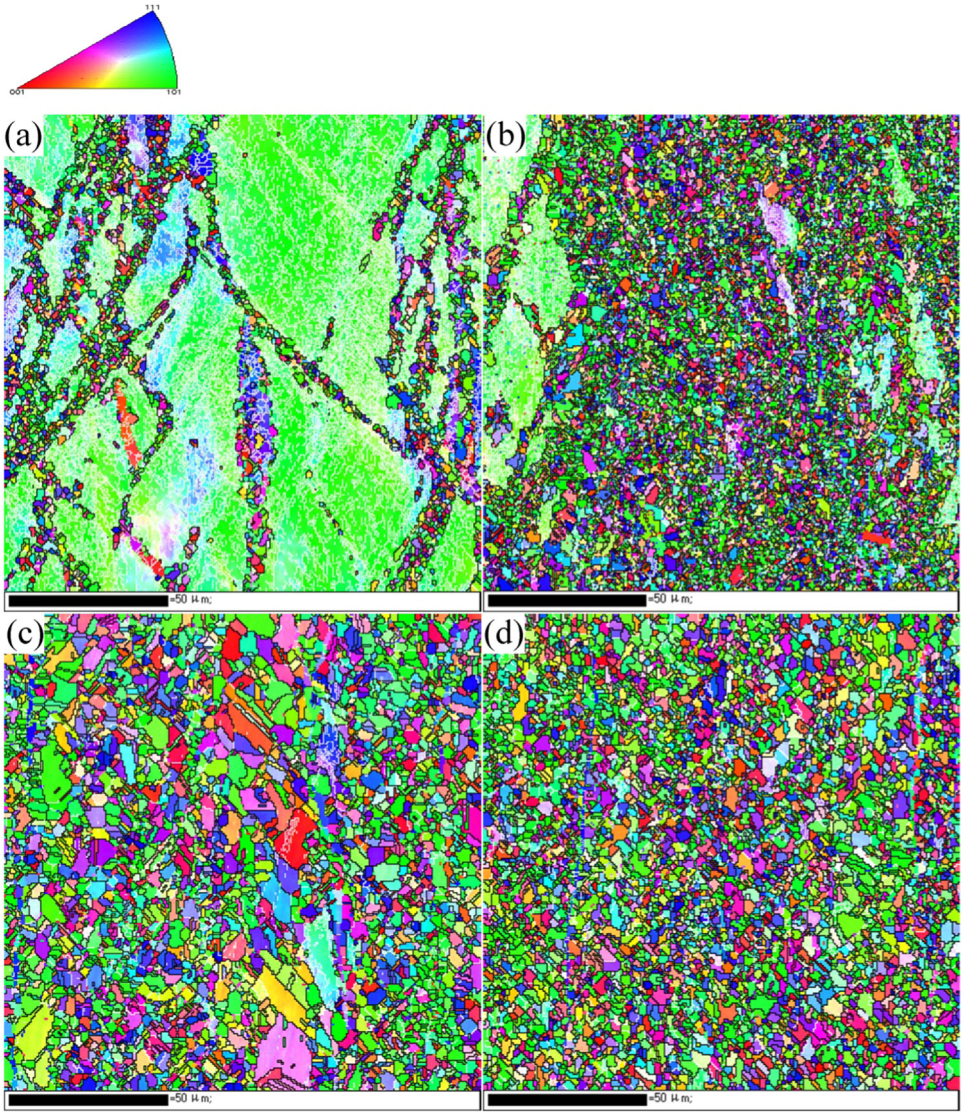

Fig. 6. Orientation map of $Al_{0.5}CoCrFeNi$ HEAs annealed at different temperature: (a) 900 °C; (b) 1000 °C; (c) 1100 °C; (d) 1200 °C.

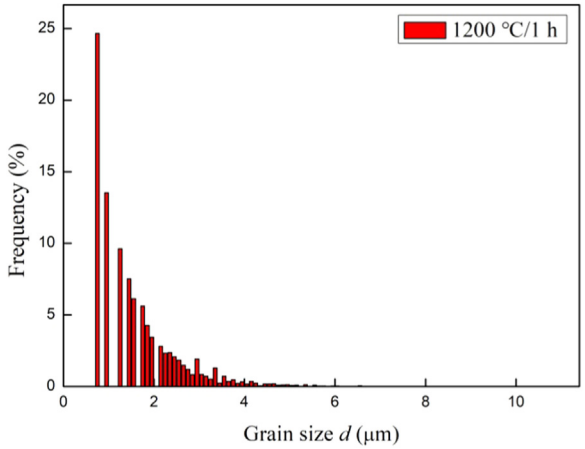

Fig. 7. Grain sizes distribution of alloy annealed at 1200 °C.

capability of $Al_{0.5}$CoCrFeNi HEA can be exploited to tune the microstructure and develop structural material with superior mechanical properties by cold rolling combined with subsequent annealing or thermo-mechanical processing as reported in other HEAs [23].

3.6. Texture analysis

In order to further illustrate and understand the effect of annealing on the microstructure of $Al_{0.5}$CoCrFeNi HEA, the textures evolution of $Al_{0.5}$CoCrFeNi HEA annealed at different temperature is determined by EBSD technique. The pole figures of alloys annealed at 900 °C and 1200 °C are shown in Fig. 8, in which the X_0 represents the normal direction (ND) and the Y_0 represents the rolling direction (RD). Alloy annealed at 900 °C with a maximum texture intensity of 23.27 shows strong {111} < 110 > and {110} < 112 > textures. As previously mentioned, the sample annealed at 900 °C retains original deformed microstructure with only a few recrystallized grains between the boundaries. Hence, the strong {111} < 110 > and {110} < 112 > textures are generated by the severely plastic deformation. Texture of sample annealed at 1200 °C with a maximum of 2.83 is arrestingly weakened through recrystallization compared with samples annealed at 900 °C, which can also be evidenced by the inverse pole figures shown in Fig. 9. In Fig. 9(a), sample annealed at 900 °C reveals < 110 > along the normal direction (ND), with < 121 > in the rolling direction (RD) and strong texture of < 111 > in the transverse direction (TD). The maximum texture intensity in other three samples annealed at 1000 °C, 1100 °C and 1200 °C with a gradually decreased tendency in Fig. 8(b) ~ (d) is 2.73, 1.78, 1.66 respectively, confirming the elimination of texture by recrystallization. Noticeable < 110 > //ND and < 111 > // RD texture components are developed after annealing which is the same with other reports [23,41]. Although the maximum intensity is decreased, the relative intensity of < 110 > //ND and < 111 > // RD texture is developing with the accomplishment of recrystallization, confirming the recrystallization texture in $Al_{0.5}$CoCrFeNi HEAs. It can be concluded from Fig. 6 that < 110 > //ND texture is related to the deformed texture while < 111 > // RD texture is independent of the original deformed texture.

3.7. Mechanical properties after annealing treatment

Microstructure changes significantly after annealing hence it is absolutely necessary to detect the mechanical properties. The tensile engineering stress-strain curves of annealed alloys are shown in Fig. 10(a). After annealing at 700 °C and 800 °C, the alloys still keep high strength but limited ductility on account of the little change of dislocation density. Recovery and formation of LAGBs are the main phenomenon during these two stages as the low annealing temperature. The uniform elongation increases to 11.44% after annealed at 800 °C for one hour, which can be attributed to the fine structure during the boundaries mentioned in Fig. 6(a). With the increasing of annealing temperature, strength continues to decrease while plasticity improves remarkably. Alloys annealed at 1200 °C possessing the fully refined recrystallized grains has a uniform elongation of 47.79%, a yield strength of 341.3 MPa and a tensile strength of 732 MPa. More specific changing tendency of yield strength, tensile strength and uniform elongation about the annealed alloys is shown in Fig. 10(b). The increasing of

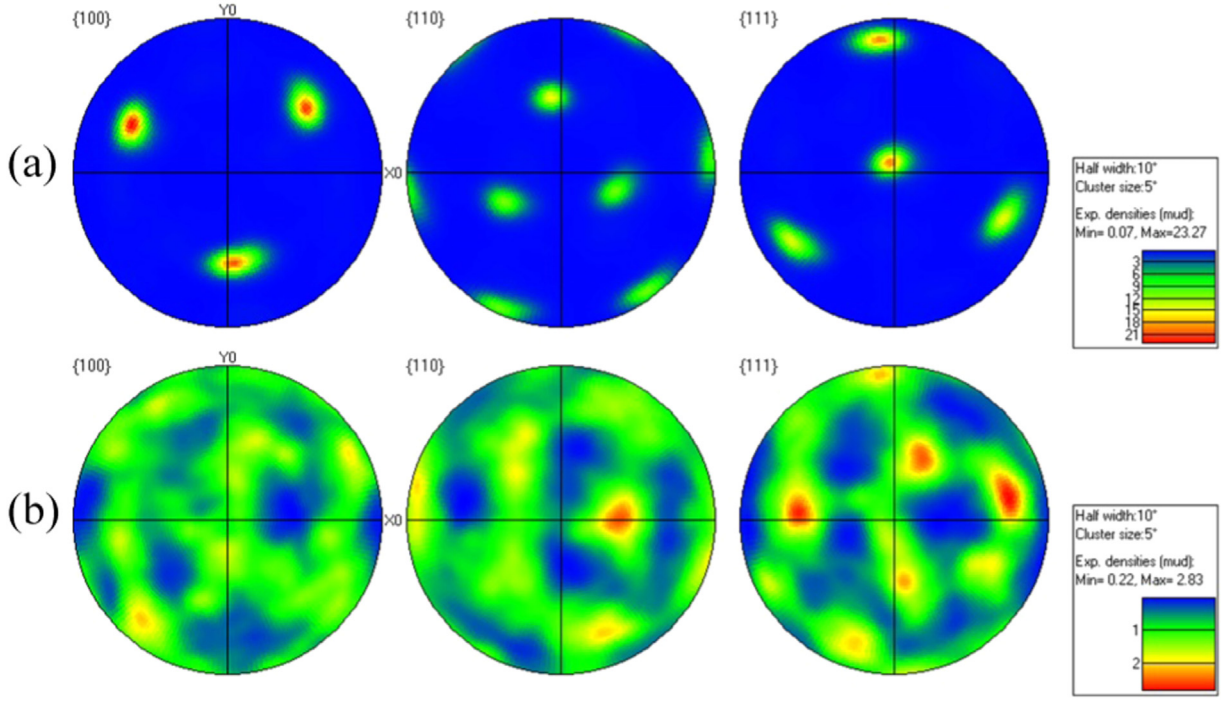

Fig. 8. Pole figures of $Al_{0.5}$CoCrFeNi HEAs annealed at different temperature: (a) 900 °C; (b) 1200 °C.

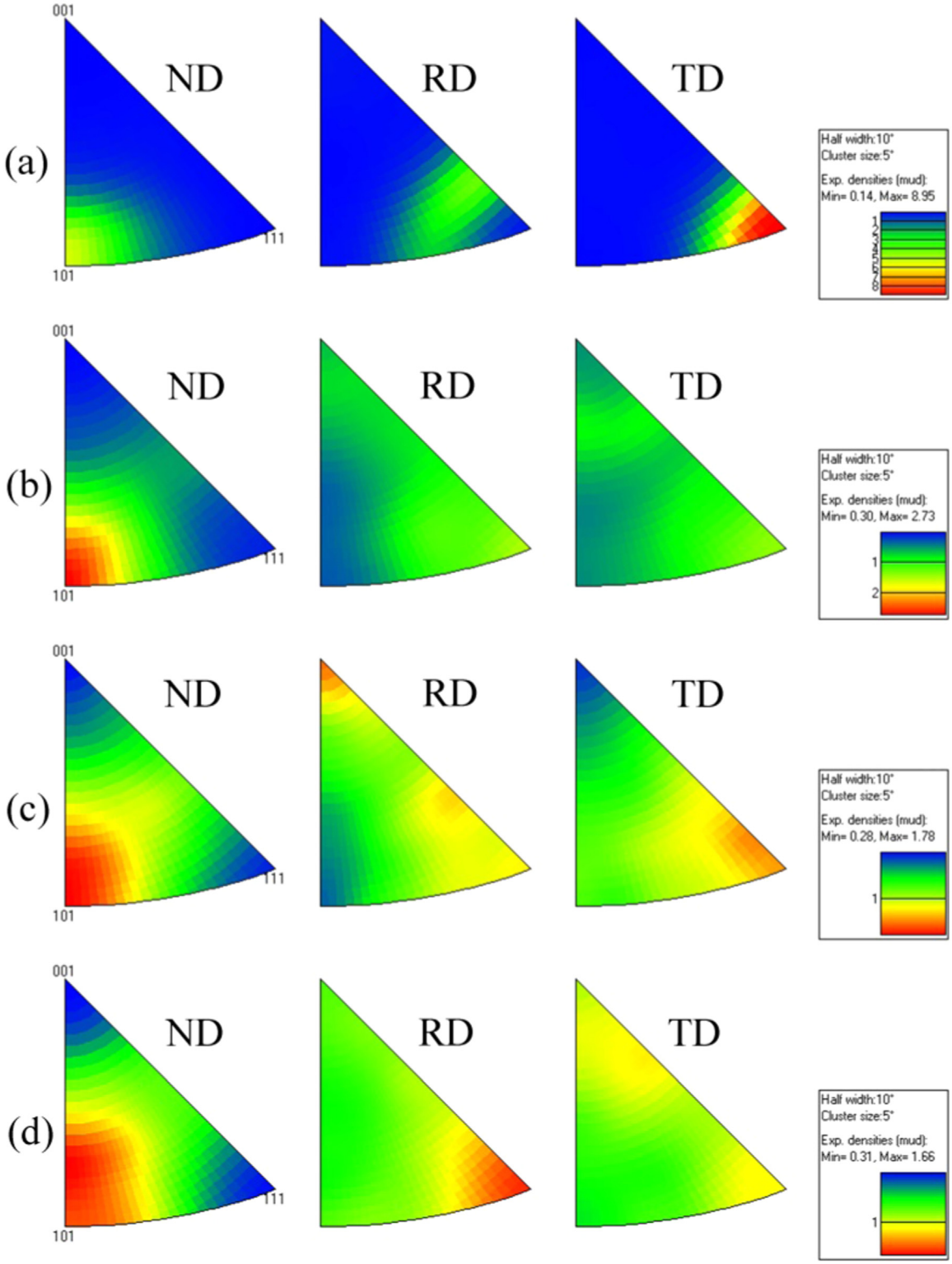

Fig. 9. Inverse pole figures of $Al_{0.5}CoCrFeNi$ HEAs annealed at different temperature: (a) 900 °C; (b) 1000 °C; (c) 1100 °C; (d) 1200 °C.

elongation and decreasing of strength can be ascribed to three factors: (1) the decreasing of dislocation density; (2) the decreasing of texture intensity; (3) the elimination of lattice distortion and strain. During the annealing process, high density dislocation turns into sub boundaries structure that translates to HAGBs and develops into recrystallization nucleation. Lacking of interactions between dislocations lowers the strength prominently. Meanwhile, high texture intensity makes material possess high strength along the RD direction. As previously mentioned in texture analysis, the strong $\{110\} < 112 >$ and $\{111\} < 110 >$ texture intensity decreases dramatically following the recrystallization which has the same changing tendency with the strength. In addition, replacement of severe deformed structure by undistorted equiaxed grains gained by recrystallization is also responsible for the changing of mechanical properties.

$Al_{0.5}CoCrFeNi$ HEAs' adjustable mechanical properties through cold rolling and subsequent annealing make it possible for many kinds of

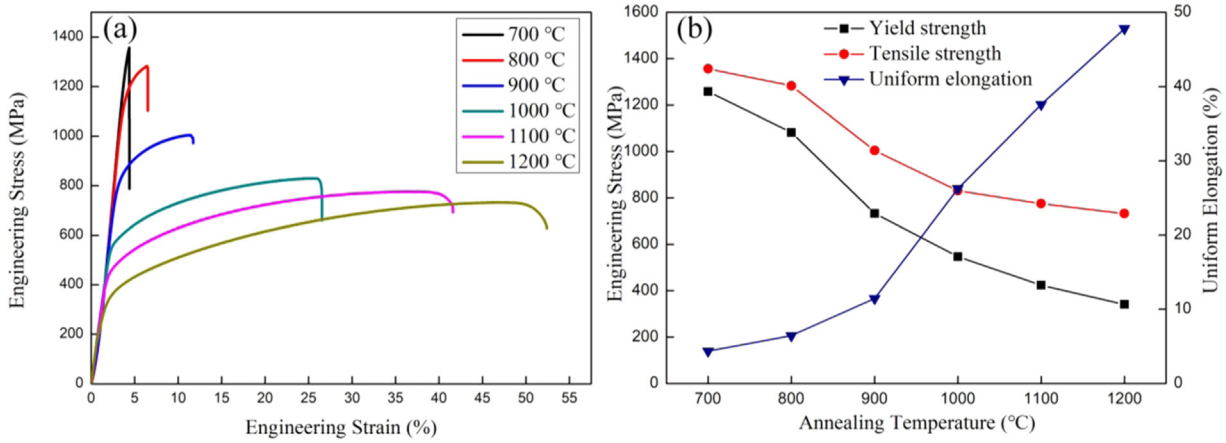

Fig. 10. Tensile properties $Al_{0.5}CoCrFeNi$ HEAs annealed at different temperature: (a) engineering stress-strain curves; (b) changing tendency of yield strength, tensile strength and uniform elongation.

applications. For example, alloys with partially recrystallization performing excellent integrated tensile properties can be used as structure materials that have been reported in CrMnFeCoNi [42] and VCrMnFeCoNi [43]. The recrystallized alloys can also be treated as the master alloys with fewer casting defects and refined grains so its integrated mechanical properties can be further improved combining with other processing method such as heat treatment. This study will be discussed in other place.

3.8. Mechanisms for extremely high recrystallization temperature

Generally, recrystallization temperature is defined as the temperature at which a particular metal with a particular amount of cold deformation (usually bigger than 70%) will completely recrystallize or nearly recrystallize (> 95%) in one hour. For pure metals the recrystallization temperature is usually 0.35–0.45 T_m (T_m is the melting point in Kelvin). According to the EBSD results shown in Fig. 6, the nearly recrystallization temperature is about 1100 °C, which is 0.81 T_m (the melting point is 1358 °C shown in Fig. 2). Such an interesting phenomenon is also reported in other HEAs like CoCrFeMnNi [23,42], $Al_{0.6}CoCrFeNi$ [25], and $Al_{0.5}CrCuFeNi_2$ [36] and $Al_{0.5}CoCrCuFeNi$ [44]. Especially, Ma et al. reported the plasticity of $Al_{0.6}CoCrFeNi$ HEA annealed at 850 °C for 1 h is unchanged, revealing a high recrystallization temperature [25]. Annealing behavior study of $Al_{0.5}CrCuFeNi_2$ HEA suggests the alloy's recrystallization temperature is about 0.8–0.9 T_m [36]. The unusual recrystallization temperature of $Al_{0.5}CoCrFeNi$ HEAs in this paper can be attributed to the following factors. Firstly the rather high recrystallization temperature is due to the coarse as-cast grains shown in Fig. 3. Coarse grains fail to resist deformation compared with fine grains therefore the distortion energy stored in cold-rolled alloys is relatively low, which reduces the driving force of recrystallization. Besides, there are less grain boundaries in coarse grains than that in the fine grains, resulting decreased nucleation sites for new grains. Hence high temperature is needed for fully recrystallization. In addition, as is known to all, HEAs have four core effects that are: (1) high-entropy effects; (2) severe lattice distortion; (3) sluggish diffusion; and (4) cocktail effects [3]. Bhattacharjee et al. think the strain energy related to severe lattice distortion in HEAs would lower the actual value of dislocation energy, stacking fault energy and grain boundary energy. As a result, driving force for recrystallization to eliminate dislocation and stacking faults is decreased correspondingly [23]. Meanwhile, the sluggish diffusion effects reported in many HEAs system [45,46] means that boundary migration is difficult in $Al_{0.5}CoCrFeNi$ HEAs because effective boundary migration requires effective atom diffusion [23]. Thus the recrystallization process needs higher temperature to motivate atom diffusion.

4. Conclusions

Bulk $Al_{0.5}CoCrFeNi$ high-entropy alloy ingot with a weight of 15.8 kg is successfully obtained by vacuum induction-melting. Cold rolling and subsequent annealing are implemented to specimens cut from bulk HEA ingot so as to eliminate foundry defects, control the microstructure as well as mechanical properties. Based on the framework above, the following conclusions are reached:

(1) $Al_{0.5}CoCrFeNi$ HEA has excellent cold workability and can be rolled at room temperature to 80% thickness reduction without any evidence of failure. The hardness, yield strength and tensile strength achieved by 80% thickness reduction are 480 HV, 1396 MPa and 1461 MPa, respectively, showing arresting work hardening effect compared with the as-cast condition.
(2) Cold rolling $Al_{0.5}CoCrFeNi$ HEA leads to hardening mainly due to the strong dislocation interactions by the dislocation accumulation. In addition, deformation twinning and lattice distortion caused by cold rolling is also responsible for the strengthening.
(3) The microstructure evolution of annealed $Al_{0.5}CoCrFeNi$ HEA from partial recrystallization to fully recrystallization is detailed described and the result indicates a high recrystallization temperature: ~ 0.81 T_m. Such a phenomenon is ascribed to coarse as-cast grains, severe lattice distortion effect and sluggish diffusion effect.
(4) The texture evolution is described by pole figures and inverse pole figures gained from EBSD measurement. The strong {110} < 112 > and {111} < 110 > texture generated by the cold rolling can be can be effectively eliminated through fully recrystallization and weak < 110 > //ND and < 111 > // RD recrystallization texture are detected.
(5) On account of the decreasing of dislocation density, the decreasing of texture intensity and the elimination of lattice distortion, strength of annealed $Al_{0.5}CoCrFeNi$ HEAs decreases dramatically and ductility increases remarkably as the annealing temperature continues to increase. In an overall view, annealed $Al_{0.5}CoCrFeNi$ HEAs possessing refined grains and adjustable tensile properties in a large scale can be used in many applications.

Acknowledgement

This work was supported by the Natural Science Foundation of China (No. 51571161 and 51774240) and the Natural Science Basic Research Plan in Shaanxi Province of China (2016JQ5003).

References

[1] J.W. Yeh, S.K. Chen, S.J. Lin, J.Y. Gan, T.S. Chin, T.T. Shun, C. Tsau, S.Y. Chang, Nanostructured high-entropy alloys with multiple principal elements: novel alloy design concepts and outcomes, Adv. Eng. Mater. 6 (2004) 299–303.

[2] C. Ng, S. Guo, J.H. Luan, Q. Wang, J. Lu, S.Q. Shi, C.T. Liu, Phase stability and tensile properties of Co-free Al0.5CrCuFeNi2 high-entropy alloys, J. Alloy. Compd. 584 (2014) 530–537.

[3] Y. Zhang, T.T. Zuo, Z. Tang, M.C. Gao, K.A. Dahmen, P.K. Liaw, Z.P. Lu, Microstructures and properties of high-entropy alloys, Prog. Mater. Sci. 61 (2014) 1–93.

[4] B. Cantor, I.T.H. Chang, P. Knight, A.J.B. Vincent, Microstructural development in equiatomic multicomponent alloys, Mater. Sci. Eng., A 375–377 (2004) 213–218.

[5] Y. Zhang, J.S. Li, J. Wang, S.Z. Niu, H.C. Kou, Hot deformation behavior of as-cast and homogenized $Al_{0.5}$CoCrFeNi high entropy alloys, Metals 6 (11) (2016) 277.

[6] Z.M. Li, C.C. Tasan, K.G. Pradeep, D. Raabe, A. TRIP-assisted, dual-phase high-entropy alloy: grain size and phase fraction effects on deformation behavior, Acta Mater. 131 (2017) 323–335.

[7] J. Wang, Y. Zhang, S.Z. Niu, W.Y. Wang, H.C. Kou, J.S. Li, S.Q. Wang, E. Beaugnon, Formation of a hexagonal closed-packed phase in $Al_{0.5}$CoCrFeNi high entropy alloy, MRS Commun. 7 (4) (2017) 879–884.

[8] Z.M. Li, K.G. Pradeep, Y. Deng, D. Raabe, C.C. Tasan, Metastable high-entropy dual-phase alloys overcome the strength-ductility trade-off, Nature 534 (2016) 227–230.

[9] M.H. Tsai, J.W. Yeh, High-entropy alloys: a critical review, Mater. Res. Lett. 2 (3) (2014) 107–123.

[10] X.Z. Lim, Mixed-up metals make for stronger, tougher, stretchier alloys, Nature 533 (2016) 306–307.

[11] J. Wang, S.Z. Niu, T. Guo, H.C. Kou, J.S. Li, The FCC to BCC phase transformation kinetics in an $Al_{0.5}$CoCrFeNi high entropy alloy, J. Alloy. Compd. 710 (2017) 144–150.

[12] Y.P. Lu, X.Z. Gao, L. Jiang, Z.N. Chen, T.M. Wang, J.C. Jie, H.J. Kang, Y.B. Zhang, S. Guo, H.H. Ruan, Y.H. Zhao, Z.Q. Cao, T.J. Li, Directly cast bulk eutectic and near-eutectic high entropy alloys with balanced strength and ductility in a wide temperature range, Acta Mater. 124 (2017) 143–150.

[13] O.N. Senkov, G.B. Wilks, J.M. Scott, D.B. Miracle, Mechanical properties of $Nb_{25}Mo_{25}Ta_{25}W_{25}$ and $V_{20}Nb_{20}Mo_{20}Ta_{20}W_{20}$ refractory high entropy alloys, Intermetallics 19 (2011) 698–706.

[14] W.H. Liu, Z.P. Lu, J.Y. He, J.H. Luan, Z.J. Wang, B. Liu, Y. Liu, M.W. Chen, C.T. Liu, Ductile CoCrFeNiMo$_x$ high entropy alloys strengthened by hard intermetallic phases, Acta Mater. 116 (2016) 332–342.

[15] J.Y. He, H. Wang, H.L. Huang, X.D. Xu, M.W. Chen, Y. Wu, X.J. Liu, T.G. Nieh, K. An, Z.P. Lu, A precipitation-hardened high-entropy alloy with outstanding tensile properties, Acta Mater. 102 (2016) 187–196.

[16] J. Wang, T. Guo, J.S. Li, W.J. Jia, H.C. Kou, Microstructure and mechanical properties of non-equilibrium solidified CoCrFeNi high entropy alloy, Mater. Chem. Phys. 210 (2018) 192–196.

[17] M.H. Chuang, M.H. Tsai, W.R. Wang, S.J. Lin, J.W. Yeh, Microstructure and wear behavior of $Al_xCo_{1.5}$ $CrFeNi_{1.5}Ti_y$ high-entropy alloys, Acta Mater. 59 (2011) 6308–6317.

[18] C.Y. Hsu, T.S. Sheu, J.W. Yeh, S.K. Chen, Effect of iron content on wear behavior of AlCoCr$Fe_xMo_{0.5}$Ni high-entropy alloys, Wear 268 (2010) 653–659.

[19] C.M. Li, H.L. Tsai, Evolution of microstructure, hardness, and corrosion properties of high-entropy $Al_{0.5}$CoCrFeNi alloy, Intermetallics 19 (2011) 288–294.

[20] D.B. Miracle, Critical assessment 14: high entropy alloys and their development as structural materials, Mater. Sci. Technol. 31 (2015) 1142–1147.

[21] Y.P. Lu, Y. Dong, S. Guo, L. Jiang, H.J. Kang, T.M. Wang, B. Wen, Z.J. Wang, J.C. Jie, Z.Q. Cao, H.H. Ruan, T.J. Li, A promising new class of high-temperature alloys: eutectic high-entropy alloys, Sci. Rep. 4 (2014) 6200.

[22] J.X. Wang, J.S. Li, J. Wang, F. Bu, H.C. Kou, C. Li, P.X. Zhang, E. Beaugnon, Effect of solidification on microstructure and properties of FeCoNi$(AlSi)_{0.2}$ high-entropy alloy under strong static magnetic field, Entropy 20 (4) (2018) 275.

[23] P.P. Bhattacharjee, G.D. Sathiaraj, M. Zaid, J.R. Gatti, C. Lee, C.W. Tsai, J.W. Yeh, Microstructure and texture evolution during annealing of quiatomic CoCrFeMnNi high-entropy alloy, J. Alloy. Compd. 587 (2014) 544–552.

[24] S.J. Sun, Y.Z. Tian, H.R. Lin, X.G. Dong, Y.H. Wang, Z.J. Zhang, Z.F. Zhang, Enhanced strength and ductility of bulk CoCrFeMnNi high entropy alloy having fully recrystallized ultrafine-grained structure, Mater. Des. 133 (2017) 122–127.

[25] L.L. Ma, L. Wang, Z.H. Nie, F.C. Wang, Y.F. Xue, J.L. Zhou, T.Q. Cao, Y.D. Wang, Y. Ren, Reversible deformation-induced martensitic transformation in $Al_{0.6}$CoCrFeNi high-entropy alloy investigated by in situ synchrotron-based high-energy X-ray diffraction, Acta Mater. 128 (2017) 12–21.

[26] H.Y. Yasuda, H. Miyamoto, K. Cho, T. Nagase, Formation of ultrafine-grained microstructure in $Al_{0.3}$CoCrFeNi high entropy alloys with grain boundary precipitates, Mater. Lett. 199 (2017) 120–123.

[27] B. Gwalani, V. Soni, M. Lee, S. Mantri, Y. Ren, R. Banerjee, Optimizing the coupled effects of Hall-Petch and precipitation strengthening in a $Al_{0.3}$CoCrFeNi high entropy alloy, Mater. Des. 121 (2017) 254–260.

[28] J.Y. He, C. Zhu, D.Q. Zhou, W.H. Liu, T.G. Nieh, Z.P. Lu, Steady state flow of the FeCoNiCrMn high entropy alloy at elevated temperatures, Intermetallics 55 (2014) 9–14.

[29] I. Baker, F.L. Meng, M. Wu, A. Brandenberg, Recrystallization of a novel two-phase FeNiMnAlCr high entropy alloy, J. Alloy. Compd. 656 (2016) 458–464.

[30] I.S. Wani, T. Bhattacharjee, S. Sheikh, I.T. Clark, M.H. Park, T. Okawa, S. Guo, P.P. Bhattacharjee, N. Tsuji, Cold-rolling and recrystallization textures of a nano-lamellar AlCoCrFe$Ni_{2.1}$ eutectic high entropy alloy, Intermetallics 84 (2017) 42–51.

[31] Y.F. Kao, T.J. Chen, S.K. Chen, J.W. Yeh, Microstrcuture and mechanical property of as-cast, -homogenized, and –deformed Al_xCoCrFeNi ($0 \le x \le 2$) high-entropy alloys, J. Alloy. Compd. 488 (2009) 57–64.

[32] S.Z. Niu, H.C. Kou, T. Guo, Y. Zhang, J. Wang, J.S. Li, Strengthening of nanoprecipitations in an annealed $Al_{0.5}$CoCrFeNi high entropy alloy, Mater. Sci. Eng. A 671 (2016) 82–86.

[33] Z.P. Lu, H. Wang, M.W. Chen, I. Baker, J.W. Yeh, C.T. Liu, T.G. Nieh, An assessment on the future development of high-entropy alloys: summary from a recent workshop, Intermetallics 66 (2015) 67–76.

[34] O.N. Senkov, S.L. Semiatin, Microstructure and properties of a refractory high-entropy alloy after cold working, J. Alloy. Compd. 649 (2015) 1110–1123.

[35] Z. Wang, M.C. Gao, S.G. Ma, H.J. Yang, Z.H. Wang, M. Ziomek-Moroz, J.W. Qiao, Effect of cold rolling on the microstructure and mechanical properties of $Al_{0.25}$CoCr$Fe_{1.25}Ni_{1.25}$ high-entropy alloy, Mater. Sci. Eng., A 645 (2015) 163–169.

[36] S.G. Ma, J.W. Qiao, Z.H. Wang, H.J. Yang, Y. Zhang, Microstructural features and tensile behaviors of the $Al_{0.5}$CrCuFeNi_2 high-entropy alloy by cold rolling and subsequent annealing, Mater. Des. 88 (2015) 1057–1062.

[37] J.Y. He, H. Wang, H.L. Huang, X.D. Xu, M.W. Chen, Y. Wu, X.J. Liu, T.G. Nieh, K. An, Z.P. Lu, A precipitation-hardened high-entropy alloy with outstanding tensile properties, Acta Mater. 102 (2016) 187–196.

[38] J.X. Hou, M. Zhang, S.G. Ma, P.K. Liaw, Y. Zhang, J.W. Qiao, Strengthening in $Al_{0.25}$CoCrFeNi high entropy alloys by cold rolling, Mater. Sci. Eng. A 707 (2017) 593–601.

[39] F. Otto, A. Dlouhy, C. Somsen, H. Bei, G. Eggeler, E.P. George, The influence of temperature and microstructure on the tensile properties of a CoCrFeMnNi high-entropy alloy, Acta Mater. 61 (2013) 5743–5755.

[40] B. Gludovatz, A. Hohenwarter, D. Catoor, E.H. Chang, E.P. George, R.O. Ritchie, A fracture-resistant high-entropy alloy for cryogenic applications, Science 6201 (2014) 1153–1158.

[41] J.X. Hou, M. Zhang, H.J. Yang, J.W. Qiao, Deformation behavior of $Al_{0.25}$CoCrFeNi high-entropy alloy after recrystallization, Metals 7 (2017) 111, http://dx.doi.org/10.3390/met7040111.

[42] J.W. Bae, J. Moon, M.J. Jang, D.M. Yim, D. Kim, S. Lee, H.S. Kim, Trade-off between tensile property and formability by partial recrystallization of CrMnFeCoNi high-entropy alloy, Mater. Sci. Eng. A 703 (2017) 324–330.

[43] Y.H. Jo, S. Jung, W.M. Choi, S.S. Sohn, H.S. Kim, B.J. Lee, N.J. Kim, S. Lee, Cryogenic strength improvement by utilizing room-temperature deformation twinning in a partially recrystallized VCrMnFeCoNi high-entropy alloy, Nat. Commun. 8 (2017) 15719.

[44] C.W. Tsai, Y.L. Chen, M.H. Tsai, J.W. Yeh, T.T. Shun, S.K. Chen, Deformation and annealing behaviors of high-entropy alloy $Al_{0.5}$CoCrCuFeNi, J. Alloy. Compd. 486 (2009) 427–435.

[45] K.Y. Tsai, M.H. Tsai, J.W. Yeh, Sluggish diffusion in Co-Cr-Fe-Mn-Ni high-entropy alloys, Acta Mater. 61 (2013) 4887–4897.

[46] J.W. Yeh, S.K. Chen, S.J. Lin, J.Y. Gan, T.S. Chin, T.T. Shun, C.H. Tsau, S.Y. Chang, Nanostructured high-entropy alloys with multiple principal elements: novel alloy design concepts and outcomes, Adv. Eng. Mater. 6 (2004) 299–303.